PAPER Nr. : 29

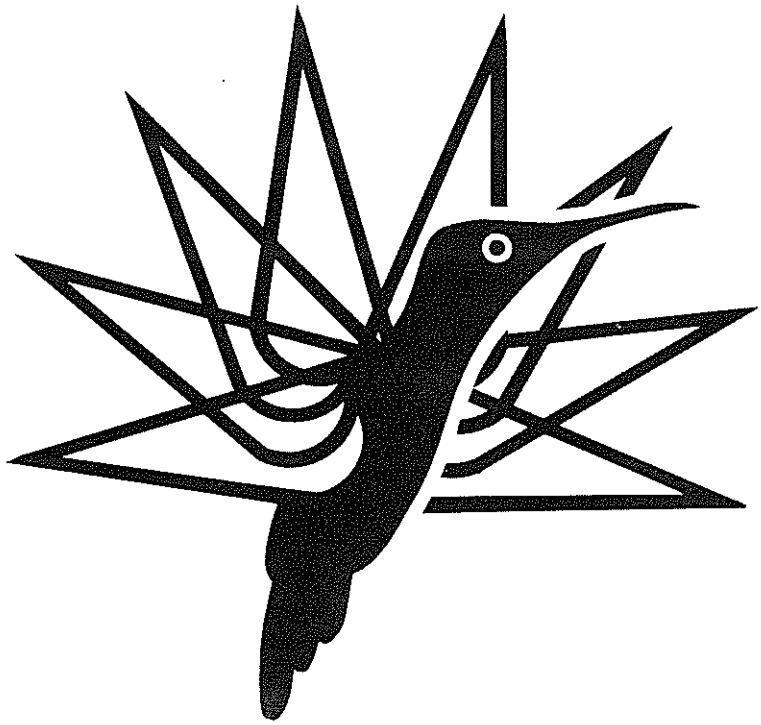

HELICOPTER FLIGHT CHARACTERISTICS IMPROVEMENT THROUGH SWEPT-TIP ROTOR BLADES

by

H. Huber

Messerschmitt-Bölkow-Blohm GmbH
Munich, Germany

FIFTH EUROPEAN ROTORCRAFT AND POWERED LIFT AIRCRAFT FORUM
SEPTEMBER 4 – 7TH 1979 - AMSTERDAM, THE NETHERLANDS

HELICOPTER FLIGHT CHARACTERISTICS IMPROVEMENT THROUGH SWEPT-TIP ROTOR BLADES

H. Huber

Messerschmitt-Bölkow-Blohm GmbH
Munich, Germany

Abstract

A theoretical and experimental program was conducted concerning the design, development and flight testing of two different types of swept-tip helicopter rotor blades. Main emphasis was placed upon simultaneous improvements of aerodynamic performance, of flight mechanics behaviour and of rotor load characteristics.

Various modifications of tip sweep, mass- c.g.-location and airfoil distributions were investigated to systematically explore the effect of main tip design parameters. Two different blade configurations were manufactured and flight tested on the BO 105 helicopter (hingeless rotor), within a speed range of up to 300 km/h and corresponding advancing tip Mach number of 0.90. Flight results showed the expected improvements in flight characteristics.

The paper presents the essential results of the blade tip design process and of flight tests. Both theoretical and experimental data will be discussed, comparing swept-tip and standard rotor blades in the areas of performance, flight characteristics and load behaviour. It is concluded that, by application of properly designed swept-tip configurations, desirable and powerful improvements in flight behaviour can be obtained.

Notation

c_D	Profile drag coefficient
c_T/σ	Rotor lift coefficient - solidity ratio
$d_{c.g.}$	Center-of-gravity offset from elastic axis
g	Gravitational constant
I_{yy}	Aircraft moment of inertia (pitch)
m	Local blade mass
M_{AT}	Advancing tip Mach number
M_T	Torsional moment
M_u	Pitching moment derivative due to forward speed, $\partial M_y/\partial u/I_{yy}$
M_q	Pitching moment derivative due to pitch rate, $\partial M_y/\partial q/I_{yy}$
M_α	Pitching moment derivative due to angle-of-attack, $\partial M_y/\partial \alpha/I_{yy}$
R	Rotor radius
t_D	Time-to-double amplitude
T	Period

Z_w	Vertical force derivative due to vertical speed, $\partial P_z/\partial w/GW/g$
β	Flap angle, positive up
Λ_{LE}	Leading edge sweep angle
μ	Advance ratio, $V/\Omega R$
σ	Rotor solidity, $bc/\pi R$
Ω	Rotor angular velocity

1. Introduction

Helicopters are currently being designed under stringent requirements to further extend their flight capability. There is no doubt that the rotor blades, owing to the wide variety of their operational conditions, are one of the prime constraining components and there is also agreement in that the blade sections near the tip do play an essential role in this respect.

In recent years, new configurations of blade tips have been repeatedly studied and a number of current helicopter designs are employing advanced tip shape modifications. Main goals of these swept-tip blades are usually concentrated on the relief of the compressible flow problems on the advancing blade, which highly affect performance, system loads and noise, for example.

In the analytical field, worldwide efforts are being undertaken to obtain a fundamental understanding of and to develop numerical methods for predicting the three-dimensional, transonic, time-dependent airflow around a rotor blade tip of arbitrary planform. Recent progress made in this field is discussed in numerous excellent papers. Citing the references (1) to (8) can only be a short survey of the related studies.

In addition to the aerodynamic problem, the dynamic and aeroelastic problems have also to be addressed, because modifications of tip planform shapes are inseparably connected with alterations in the mass locations of the rotor blade structure. In this respect, the offset of center-of-gravity, with resulting mechanisms of aeroelastic bending-torsion couplings, is only one influential parameter, as has been discussed in References (9), (10), for example.

At Messerschmitt-Bölkow-Blohm an analytical/experimental program, sponsored by the Ministry of Defence of the Federal Republic of Germany, was conducted to investigate advanced swept-tip rotor blade concepts employing aeroelastic-feedback characteristics. The main goals were oriented to performance and flight characteristics improvements, with special consideration of the MBB hingeless rotor system. Figure 1 shows a double-swept tip configuration, designed and flight tested on a BO 105 helicopter during this program. Figure 2 shows a redesigned blade version with a progressive sweep-tip shape, which was also flight tested.

The paper will shortly describe the approach taken in addressing the basic swept-tip design problem, and will present theoretical and flight test results for the two blade configurations. Main conclusions will be drawn from comparison with the standard blades.

2. Method of Analysis

To obtain an "in depth" understanding of the rotor phenomena, appropriate physical modelling of both the airflow around the rotor blades and of the dynamic and aeroelastic response is necessary. This is especially true for swept-tip blade versions, as aerodynamic and mass forces are acting on increased moment arms relative to the blade's axes (Figure 3), thus affecting the main response characteristics considerably. To describe the strongly interfering aerodynamic and aeroelastic phenomena, within a universal flight dynamic theory, requires a highly "matched" model without excessively sophisticated theories in the individual disciplines.

2.1 Blade Aerodynamic Calculation

The aerodynamic model used for the subsequent studies of swept-tip configurations is a modification of blade element theory. Under the aspects discussed above, the effects of tip sweep are modelled with simplifying assumptions. Taking into account recent results (References (1), (4)) showing certain effects of three-dimensional aerodynamic "de-sweeping" on swept-tips, the following assumptions are made: The effective free stream velocity (dynamic pressure) at the swept elements is equivalent to the component of the non-swept tip; spanwise velocity is ignored. The effective Mach number on a swept element is considered as

$$M_{\text{Swept Element}} = M_{\text{Straight Element}} \cdot (\cos \Lambda)^{1/2} \quad .$$

The effective angle-of-attack resulting from the free-stream and rotor induced flow conditions is considered not to be influenced by sweep angle. For actual angles and Mach numbers (reduced), the airfoil characteristics are taken from 2-dimensional, steady airfoil data, including stall and compressibility effects from tests. Unsteady aerodynamic effects are not included in this analysis, since they have been found to be generally small for flight dynamic and rotor stability considerations.

The geometric blade modelling is shown in Figure 4. It includes arbitrary spanwise distributions of geometric and aerodynamic tip parameters, i.e. blade chord, twist, aerodynamic center position, leading edge sweep, and airfoil sections. The local built-in offset of the aerodynamic center can be selected by considering the three-dimensional effects near the tip.

2.2 Blade Dynamic Calculation

As already mentioned, in addition to the aerodynamic effects of sweep-relief and a.c.-offset, sweep-back of aerodynamic surfaces also means an offset of real mass elements relative to the pitch and elastic axes (see Figure 3). It will be illustrated in the subsequent sections, that the offset of the center-of-gravity is inherently connected with an alteration of torsional moments and corresponding torsional deflections; they are shown to be a prime factor for aerodynamic, loads, and flight dynamic effects.

As far as the blade motions are concerned, the elastically cantilevered blades of the hingeless rotor are represented by use of the

"equivalent system" technique, as reported in Reference (9), for example. As well as the flap and lag degrees of freedom, the inclusion of the torsional flexibility is of paramount importance, especially for swept-tip configurations. The physical model of the blade, shown in Figure 4, treats the discontinuous mass situation of swept-tips by an arbitrary distribution of local mass and chordwise center-of-gravity position relative to the elastic axis. One way of affecting the torsional response of swept-tip rotor blades which should be underlined here, is by the flap-bending-torsion coupling, introduced through blade sections which show a mass-center-offset relative to the elastic axis. The torsional moment is expressed by

$$M_T = \Omega^2 \left(\int_{\text{Root}}^{\text{Tip}} r \cdot \frac{dm}{dr} \cdot d_{c.g.}(r) \cdot dr \right) \cdot \sin \beta$$

It follows primarily from this equation that swept-tip sections are particularly active in producing this type of coupling, because they are inherently subject to high centrifugal mass forces owing to their long radius arm from the rotor center. The fundamental mechanisms of torsion, owing to blade bending, and the significant influences of the chordwise mass-c.g. location on this type of aeroelastic coupling, have been reported in References (9) and (10).

3. Analytical Investigations

3.1 Configurations Studied

To gain a fundamental understanding of the influences resulting from blade tip modifications, a systematic analytical study was initially conducted. The BO 105 helicopter, with the hingeless rotor, served as the baseline rotorcraft. Some important rotor data are described in Figure 5.

The blade configurations studied are illustrated in Figure 6. The BO 105 standard blade has a straight, untapered planform with a constant NACA 23012 (modified) airfoil section. The blade shows constant mass distribution (5.6 kg/m) with a corresponding mass center-of-gravity location of about 24.7% of chord. This baseline blade was studied in modified versions. The leading edge was varied between $+30^{\circ}$ (aft-sweep) and -30° (fore-sweep) in the outer 7.5% of radius and between $+20^{\circ}$ and -20° in the outer 12.5% of radius. Chord, airfoil, and mass distributions were equivalent to the baseline blade.

A second tip shape modification is illustrated in the right half of Figure 6. Blade external characteristics show a double swept, tapered tip planform with the leading edge sweep angle being varied between 22° and 38°. The airfoil section is tapered from NACA 23012 mod. to a 6% airfoil. To combine the individual effects of built-in offset of aerodynamic center and of mass-c.g., appropriate mass characteristics were chosen, see Figure 7. Blade mass is increased in the fore-sweep section with corresponding c.g.-forwardshift and is reduced in the aft-sweep section outside of 0.92 R.

3.2 Evaluation of Aerodynamic and Aeroelastic Mechanisms

Drag Reductions - Based on the simple model assumptions for the tip aerodynamics, the variation of drag coefficient with span at the advancing side position ($\psi = 90^{\circ}$) is shown in Figure 8 (advance ratio 0.35, advancing tip Mach number 0.88). The baseline untapered, unswept-tip blade is compared to two blades with modified tips, AGB I and AGB III. The blade with reduced-in-thickness tip shows considerable reduction in the outer 15% of rotor radius. The second blade version, including a 30° tip sweep in combination with chord and airfoil taper, shows considerably less drag in the outer blade portion. It should be noted, however, that at positions inboard of about 85% of radius the drag coefficient increases, although the blade characteristics are identical to the baseline blade in this section.

The explanation can be obtained by considering differences in the torsional response of the different blade versions. The lift distribution versus span in high speed conditions shows negative thrust at the advancing blade tip. This local download is acting on the positive arm of the aft-swept tip, thus producing a positive torsional moment which, by virtue of the torsional flexibility of the blade, increases the angle-of-attack. Although the negative thrust of the tip itself is reduced by this mechanism, the blade is positively twisted, and hence, the angle-of-attack at the more inboard stations is increased, producing a local drag increase as indicated in Figure 8.

Dynamic Lift Variation - The alteration of the azimuth lift distribution discussed above is shown in Figure 9, on the example of the double-swept tip version. The torsional elastic deflections are also shown, clearly indicating the controlling mechanism of the torsional response to the blade thrust variation. With 30° sweep angle the predominant second harmonic blade lift variation, which is typical for forward flight conditions, is reduced by about 60%, when compared with the unswept blade. Conversely, studies on blade variations with fore-sweep-tips have shown that fore-sweep would increase dramatically the oscillating blade lift components.

The beneficial effect of a dynamic reduction in the fluctuating lift forces by tip aft-sweep is of high importance not only for blade stresses, but also under the aeroacoustic aspect. Noise calculations based on the airloads of Figure 9 have indicated that a sound pressure reduction of 2 to 4 dB in the second through fourth harmonics can be expected for the rotor with 30° swept-tip rotor blades.

Flight Dynamic Characteristics - To obtain clear understanding of the extent to which the basic flight dynamic characteristics can be altered by tip modifications, principal studies have been conducted considering the swept-tip modifications of the BO 105 standard blade (see Figure 6). The fact that the tip section shows constant chord, constant airfoil and constant mass distribution, enables a clearer understanding and interpretation of the individual effects.

Basic influences on longitudinal stability derivatives are shown in Figure 10 for a typical medium speed (200 km/h). The diagram illustrates the effects of variations in sweep angle from $+30^{\circ}$ to -30° and of varying the position at which a fixed sweep angle begins. Note that the results

of Figures 10 and 11 are valid for blade versions having constant mass distributions in the tip section. Three important conclusions can be drawn from Figure 10:

- Aft sweep (including sweep of aerodynamic planform and local mass) shows a trend to increase the positive (i.e. unstable) angle-of-attack derivative (M_α), fore-sweep leads to a stable M_α-derivative. This trend is the more pronounced, the more inboard the sweep starts.

- Blade tip sweep is of high influence on the inherent speed-stability derivative (M_u), with M_u-values increasing for aft-sweep blades and decreasing with fore-sweep-blades. There is a tendency to negative (divergent) M_u-values with fore-swept blade tips.

- Angular velocity damping derivative M_q (not shown in Figure 10) is only to a minor extent influenced by blade sweep, with a slight tendency of increasing M_q with aft-sweep angles.

By analysing these results, the individual contribitions of aerodynamic and mass forces to changes in stability derivatives can be clearly identified. In the M_α-derivative the pure aft-sweep of aerodynamic blade area is stabilizing, because the lift increase at positive angle-of-attack change produces a negative torsional moment which twists the blade down. Conversely, the pure offset of blade mass behind the elastic axis produces a positive torsional moment, when the rotor attitude (and in consequence the flap coning angle) is increased, thus increasing the angle-of-attack instability of the rotor (both effects have in principle been reported in References (9) and (10)). In the case of the speed stability (Figure 10 bottom), both aft-shifting of aerodynamic blade area and aft-shifting of local blade mass are changing the values in a positive direction. The net result depends on the relative magnitude of these two basic influences.

Figure 11 shows the dynamic characteristics in terms of time-to-double amplitude and period as a function of tip sweep angle and of the spanwise sweep poisition. Note the degradation of dynamic stability which occurs when blades (having constant mass distribution) are swept aft. It should be further noted that a change to negative speed stability may occur with fore-sweep blades. With the elastic deflections being proportional to the torsional flexibility, the effects are more pronounced with lower torsional stiffness of the blades.

3.3 Design of Proper Swept-Tips

Based on the results it can be derived that, from the flight dynamic standpoint, proper aerodynamic shaping and mass balance have to be applied on swept-tip rotor blades. Variations of parametric data were investigated to evolve the blade layout which could provide the greatest benefit in general flight dynamics behaviour. Figure 12a shows various parameters influencing the derivatives of speed stability and angle-of-attack stability at high forward speed conditions (V = 275 km/h). The results are summarized in a comprehensive plot of speed stability derivative (M_u) vs. a maneuver-parameter ($Z_w \cdot M_q - M_\alpha$), which represents the spring term in the short period mode. Lines of constant time-to-double amplitude are indicated in the diagram. An explanation of the different parametric variations in tip sweep, airfoil section, c.g.-location and mass-distribution is given in the table of Figure 12. The most important conclusions evident from Figure 12a are:

- Reduction of airfoil thickness at the blade tip has a destabilizing influence, mainly on angle-of-attack stability

- Variations in sweep angle (see blade version 2, 3, 4) mainly affect speed stability, and have almost no influence on the M_α-axis

- Change of chordwise center-of-gravity (see blade version 2, 7, 9) mainly influences the M_α-Derivative, and has no influence on speed stability. Reducing blade sweep angle from 30° to 22° (version 10) tends to drive the stability characteristics towards the stable region in this case.

Corresponding influences on the longitudinal motions period are illustrated in Figure 12b. It should be noted that the motion becomes divergent when either M_u becomes negative, or when too high an angle-of-attack instability occurs. Blade tip parameters have to be selected while avoiding these critical areas.

Figures 13 and 14 show the predicted trends of two important stability derivatives of the AGB III blade concept versus flight speed. Comparison with the square-tip standard blade indicates that clear improvements are achieved in the M_α-derivative, while keeping the speed stability at a moderate positive level.

4. Flight Test Programs

4.1 Blade Versions Tested

Based on the analytic design studies, two blade configurations were selected for manufacturing and subsequent flight testing:

AGB III - The blade, shown in Figure 1 on the whirl test stand, has a double-swept, tapered planform with a leading edge sweep angle of 30°, starting from 87% of radius. The airfoil is tapered from NACA 23012 mod. at 0.87 R to V 13006 - 0.7 at 1.0 R. The blade is mass-overbalanced relative to the 25%-line through a concentrated (1 kg) tip weight at 0.91 R and through reduced mass in the aft-sweep section (mass-distribution see Figure 7).

In order to make the experimental blade cost effective, a special fabrication procedure had to be developed. The inboard standard blade section was pre-fabricated with the spar being extended into the tip area. The tip section was subsequently laminated in a seperate mould and was adhesively bonded to the spar and skin of the inboard section. Figure 16 gives an impression of this manufacturing process.

AGB IV - This blade configuration, shown in Figure 2 on the BO 105 test aircraft, has various modifications in comparison with the first version. The blade (Figure 15) employs a progressively swept-tip starting at 93% of radius with maximum leading edge of 30° and a trailing edge fore-sweep of 8°. The tip is tapered (taper ratio 0.4) at the outer 7% of radius. Airfoil distribution shows constant NACA 23012 mod. profile up to 0.87 R, a linear taper to V 23010 - 1.58 airfoil at 0.93 R, being constant up to blade tip. The mass distribution (see Figure 7), shows reduced mass in the aft swept region, the blade is mass-overbalanced relative to 1/4-line through slightly higher running mass in the homogenous part of the blade.

In order to provide the desired torsional stiffness in the tip section, crossplied carbon fibre was used for the build-up of the blade skin at the outer 12% of radius. The manufacturing concept was based on the application of a mould-insert into the tip section of the standard blade mould.

Fundamental dynamic characteristics of the two swept-tip rotor blades are summarized in the Table of Figure 17.

4.2 Test Vehicle and Test Program

Flight tests have been carried out on the BO 105-HGH experimental helicopter. From earlier flight test programs, reported in References (11), (12), comparative data was available for two different types of non-swept, non-tapered rotor blades, the BO 105 standard rotor blade with constant NACA 23012 mod. airfoil section, and a thin tip blade (AGB I).

There were two flight test phases for the two different blade configurations. The test program of the AGB III blades (1975) was performed at two gross weights, 1900 kg and 2300 kg. Flight speeds were investigated up to 300 km/h, which corresponds to an advance ratio of 0.38 and advancing blade Mach number of 0.90 with load factors up to 2.2 g (c_T/σ = 0.17). Flight tests of the AGB IV blade configuration commenced in 1978. With an aircraft gross weight of 2300 kg, a maximum speed of 305 km/h was achieved, which corresponds to a 0.39 advance ratio and a 0.905 advancing blade Mach number.

5. Test Results and Discussions

5.1 Power Comparison

As mentioned before, within the program investigating advanced swept-tip rotor blades, main emphasis was placed upon the evaluation of improvements in the general flight characteristics. Therefore, power measurements were not conducted to the extent necessary to provide full reliable data within a minimum scatter band. Power data, therefore, should be considered with some caution. Figure 18 shows the power comparison for two swept-tip blade configurations. The figure indicates power reductions of 3% to 5%, compared to the standard blade. For lower gross weights, these results could not be completely substantiated, therefore, a dependency upon rotor thrust must be assumed.

5.3 Control Loads

The test results did confirm the pre-test predictions of the effects of variation in blade tip parameters. Figure 19 shows typical control load characteristics for a medium speed condition of 240 km/h (advance ratio 0.30, Mach number advancing blade 0.84). Evidently, main differences between the two blades exist in the second-harmonic content of the swept-tip blade. In the foregoing discussion, this behaviour has been attributed to the effect that the download at the advancing blade tip is acting on the tip's aerodynamic center, which is aft of the pitch axis, thus causing a positive torsional moment. This same effect, in combinations with the mass-overbalance of the swept-tip configuration, gives

rise to an increase in the static control load. This is especially true for flight conditions with high positive load factors, where increasing tip thrust and aerodynamic coning angles can result in relatively high static loads. It should be mentioned that this is not a critical problem in terms of fatigue damage, especially when peak loading remains below the endurance limits. Furthermore, various means are available for reducing static pitch link loads.

5.3 Flight Characteristics

Control Behaviour - Rotor trim angles are influenced, owing principally to the change of elastic pitch by torsion resulting from built-in offset of the aerodynamic and mass center from the elastic axis. An increase of the collective pitch in horizontal flight of about 2.5 degrees for the AGB III version and of about 1.5 degrees for the AGB IV version was measured. The amplitude of the longitudinal cyclic pitch required for trim is influenced by a cyclic twist effect mainly resulting from a sweep-induced nose-up twist near the advancing blade side. Thus, the longitudinal control position vs. speed in Figure 20 is slightly more forward, indicating improved speed-stability characteristics. Studies on swept-tip rotor blades in Reference (13) show comparable results.

Dynamic control characteristics are also influenced owing to the fact that the rotor angular damping of the swept-tip blades with positive c.g.- a.c.-offset is increased. A reduction of the aircraft's rate response to stick input of about 25 percent (AGB III) and 7 percent (AGB IV) is seen from the flight test results. For a production blade design this has to be taken into account when selecting control ratios.

Longitudinal Stability - Flight test results of the double-swept blades are illustrated in Figure 21, showing the time-to-double amplitude and the period of the longitudinal motion (gross-weight 1900 kg, medium c.g.-position). It is noted that pitch stability improved significantly with this blade concept. For example, at a 200 km/h flight speed, the time-to-double amplitude was increased from about 6 sec to a level of 30 sec and the motion's period increased by about 5 sec, when compared with the standard-tip blades. The total effect of this blade configuration is to shift the speed range of "equivalent stability characteristics" by in increased 60 km/h.

A stability comparison between both swept-tip configurations and the baseline blade is presented in Figure 22, for maximum gross weight of 2300 kg. The trend of stability improvements is evident for both blade configurations. Note that, for the AGB IV with reduced sweep and c.g. overbalance, dynamic stability values are lower than for AGB III, but still consistently better than for the standard blades.

5.4 Side Effects

During flight testing of the two swept-tip blade configurations, some problems were encountered relating mainly to the vibratory behaviour of the rotor system. During specific flight conditions of low speed transition and landing approach to hover, a relative increase of dynamic control loads and aircraft vibration level was observed. Marked differences were found especially for the AGB III-version, which incor-

porates relatively large mass-variations in the tip section. The differences can confidently be attributed to an alteration of the higher-harmonic bending-torsional coupling characteristics. It is known that coupled mode frequencies and amplifications are strongly influenced by mass distribution discountinuities and that tip sections are particularly sensitive in this respect. It must be remembered that optimization of the two experimental blade versions, with respect to higher-harmonic coupling characteristics, was beyond the scope of the program conducted. Further investigation is required, and attention will have to be given, to these questions for a future production swept-tip blade design.

6. Conclusions

An analytical/experimental program was conducted investigating advanced swept-tip blade configurations on a hingeless rotor system. Based on analyses and flight testing, the following conclusions can be drawn:

- Planform sweep must be generally considered with regard to aerodynamic and dynamic mass forces, both affecting the aeroelastic response of the rotor blades.
- Through a dynamic alteration of the torsional response, local aerodynamic flow conditions are influenced. By virtue of a redistribution of airloads, the second harmonic blade loading in forward flight is significantly reduced. However, the reduction of compressible drag owing to sweep can be relatively diminished.
- Tip sweep substantially affects flying qualities, the effects being dependent upon the ratio of aerodynamic swept areas to tip swept mass. Aerodynamic sweep mainly influences speed stability with only minor effect upon angle-of-attack stability. Mass distribution and chordwise c.g. sweep mainly affect pitch-up-stability, whilst retaining speed stability unchanged.
- Through application of proper aerodynamic planform sweep and adequate mass-balance, powerful improvements in flight stability characteristics can be obtained.
- The analytical model applied is capable of reliably predicting the global effects of tip sweep modifications. The most important findings from analytical investigations were verified through flight test results. However, further modelling progress - especially in 3-dimensional tip aerodynamics - is necessary to further help in the design of future high speed rotors.

7. References

1) W.F. Ballhaus and F.X. Caradonna, The Effect of Planform Shape on the Transonic Flow Past Rotor Tips, AGARD Conf. Proc. on Aerodynamics of Rotary Wings, No. 111, Marseilles, Sept. 1972

2) F.X. Caradonna and M.P. Isom, Numerical Calculation of Unsteady Transonic Potential Flow Over Helicopter Rotor Blades, AIAA Journal, Vol. 14, No.4, April 1976

3) F.X. Caradonna and J.J. Philippe, The Flow Over a Helicopter Blade Tip in the Transonic Regime, Proceedings of the 2nd European Rotorcraft and Powered Lift Aircraft Forum, Bückeburg, Sept. 1976

4) B. Monniere and J.J. Philippe, Aerodynamic Problems of Helicopter Blade Tips, Proceedings of the 3rd European Rotorcraft and Powered Lift Aircraft Forum, Aix-en-Provence, Sept. 1977

5) J. Grant, The Prediction of Supercritical Pressure Distributions on Blade Tips of Arbitrary Shape over a Range of Advancing Blade Azimuth Angles, Proceedings of the 4th European Rotorcraft and Powered Lift Aircraft Forum, Stresa, Sept. 1978

6) M.E. Tauber, Analytic Investigation of Advancing Blade Drag Reduction by Tip Modifications, 34th Annual National Forum of the American Helicopter Society, May 1978

7) R.H. Stroub, Full-Scale Wind Tunnel Test of a Modern Helicopter Main Rotor - Investigation of Tip Mach Number Effects and Comparison of Four Tip Shapes, 34th Annual National Forum of the American Helicopter Society, May 1978

8) J.P. Rabbott, Jr. and Ch. Niebank, Experimental Effects of Tip Shape on Rotor Loads, 34th Annual National Forum of the American Helicopter Society, May 1978

9) G. Reichert and H. Huber, Influence of Elastic Coupling Effects on the Handling Qualities of a Hingeless Rotor Helicopter, AGARD Conference Proceedings on Advanced Rotorcraft, No. 121, Vol. I, Hampton Va., Sept. 1971

10) H.B. Huber, Effect of Torsion-Flap-Lag Coupling on Hingeless Rotor Stability, 29th Annual National Forum of the American Helicopter Society, May 1973

11) H. Huber and H. Strehlow, Hingeless Rotor Dynamics on High Speed Flight, First European Rotorcraft and Powered Lift Aircraft Forum, Southampton, Sept. 1975

12) H. Huber, C. Schick, A. Teleki, Hochgeschwindigkeitserprobung des Hubschraubers BO 105-HGH, 9. DGLR-Jahrestagung, München, Sept. 1976

13) G.S. Doman, F.J. Tarzanin and J. Shaw Jr., Investigation of Aeroelastically Adaptive Rotor-Systems, American Helicopter Society Mideast Region Symposium on Rotor Technology, August 1976

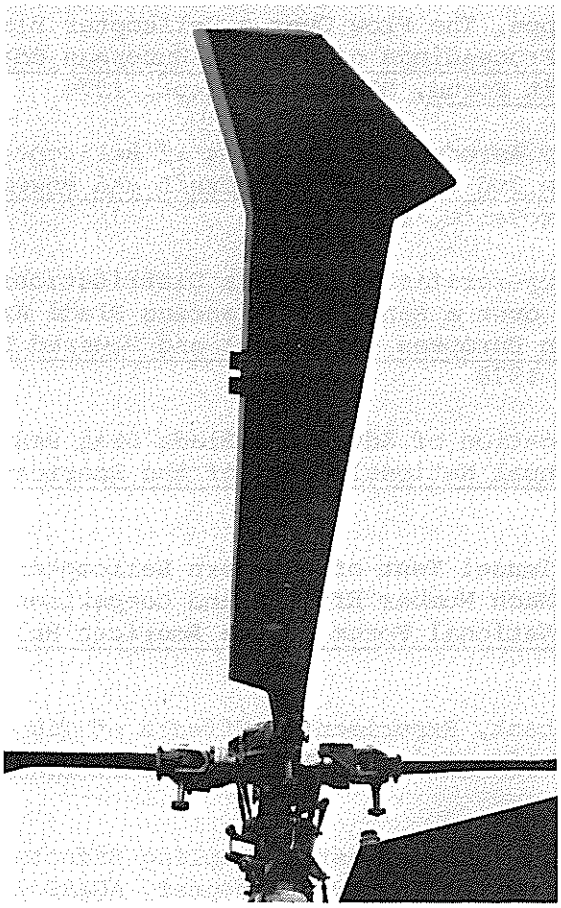

Figure 1 Advanced Geometry Blade (AGB III) on Whirl Test Stand

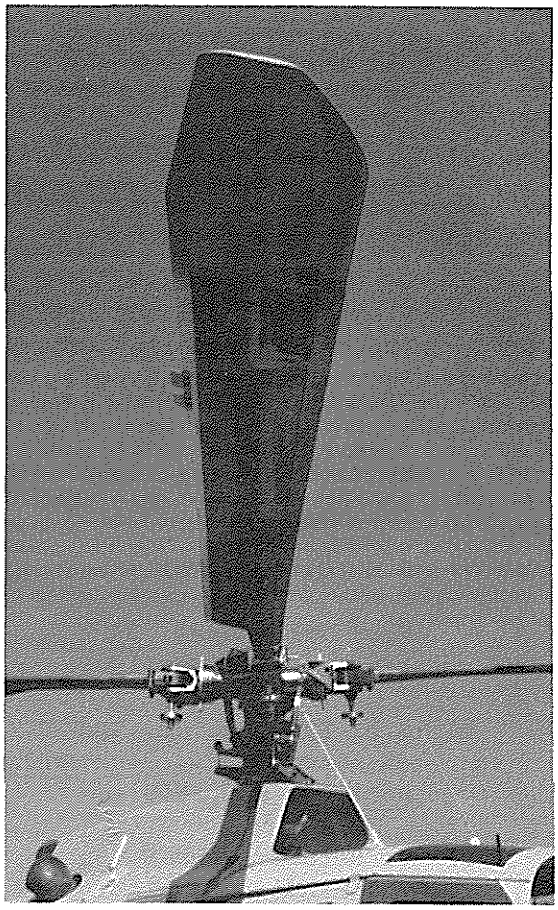

Figure 2 Advanced Geometry Blade (AGB IV) on BO 105-HGH Test Aircraft

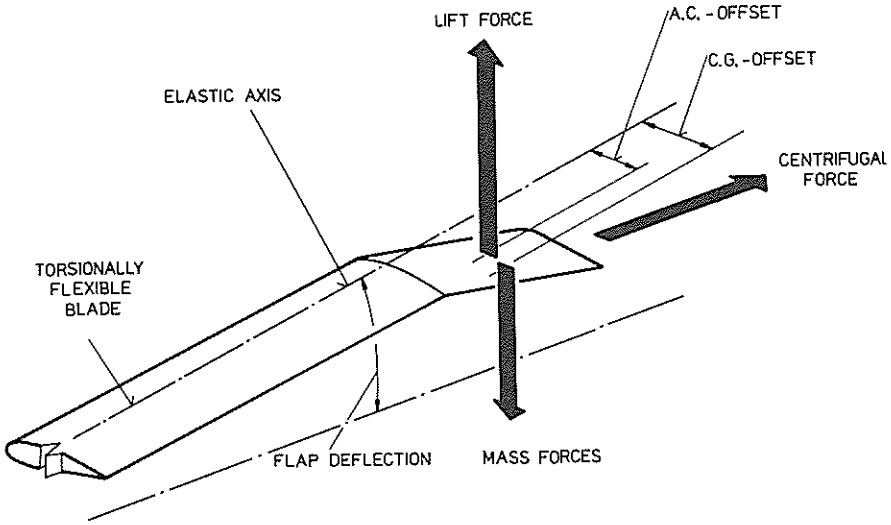

Figure 3 Torsional Moment Contributions of Swept-Tip Sections

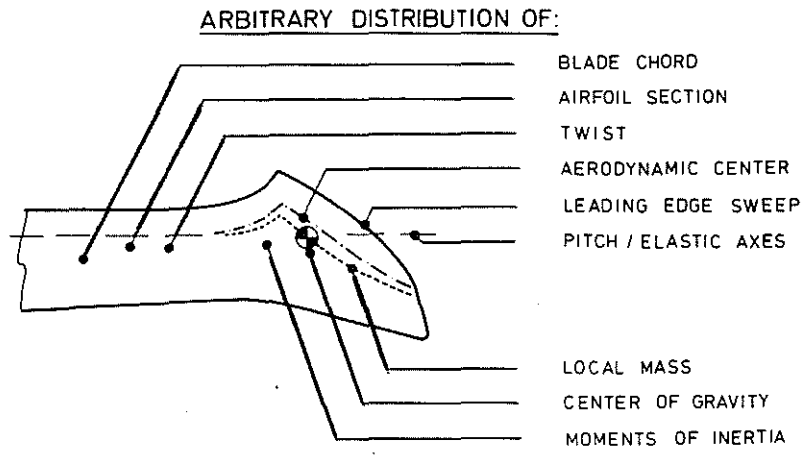

Figure 4 Physical Modelling of Swept-Tip Blade Configurations

ROTOR TYPE	HINGELESS	
DIAMETER	9.82	m
TIP SPEED	218	m/s
NUMBER OF BLADES	4	-
SOLIDITY	0.07	-
PLANFORM	RECTANGULAR	
TWIST	-8	deg
AIRFOIL	NACA 23012	(mod.)
FIRST FLAP FREQUENCY	1.117	Ω
FIRST INPLANE FREQUENCY	0.667	Ω
FIRST TORSIONAL FREQUENCY	3.7	Ω

Figure 5 BO 105 Hingeless Rotor Characteristics

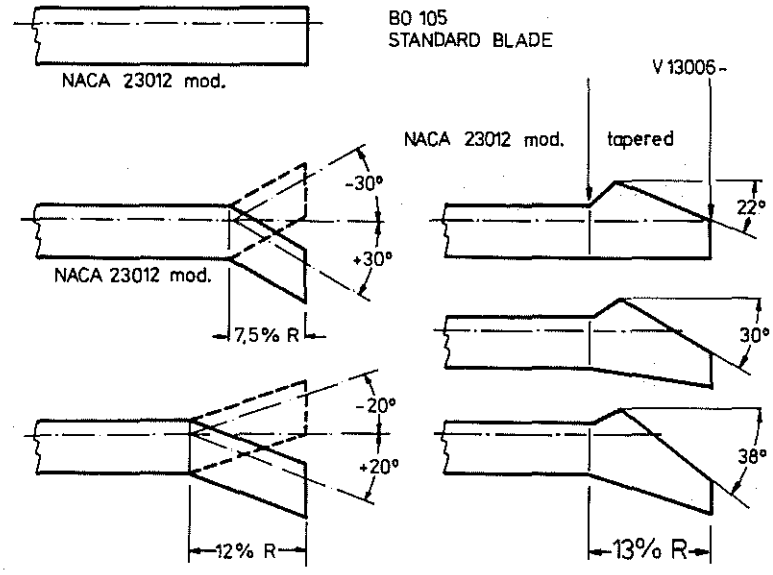

Figure 6 Swept-Tip Configurations Studied

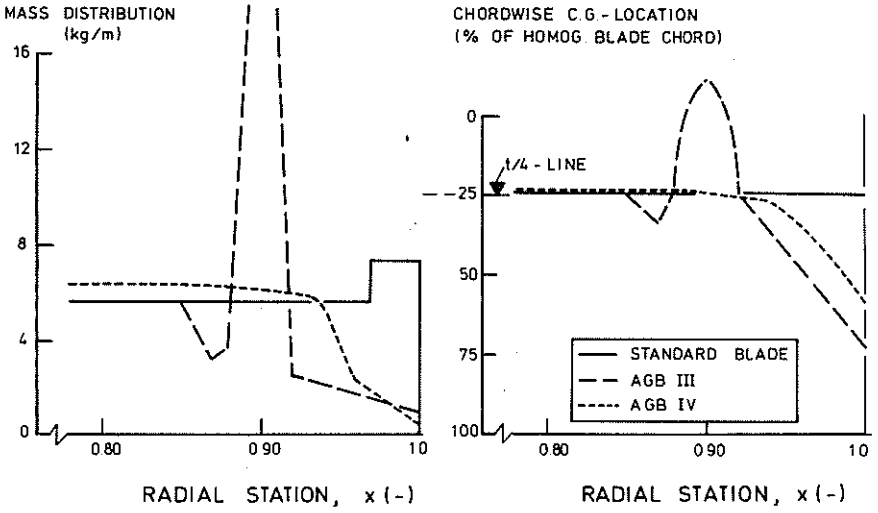

Figure 7 Blade Mass Characteristics of Swept-Tip Sections

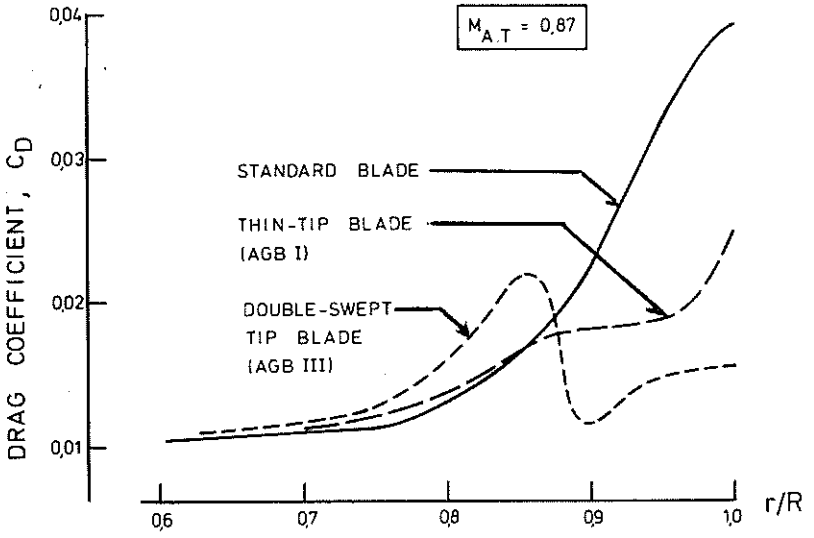

Figure 8 Local Drag Coefficient Comparison

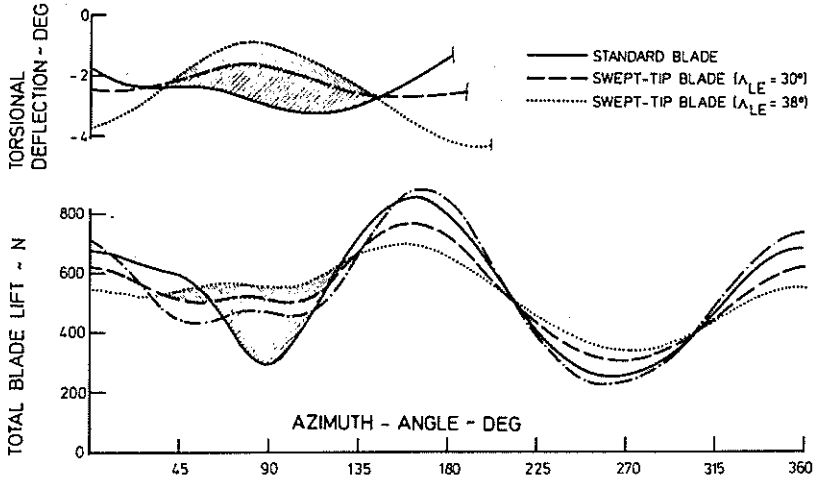

Figure 9 Dynamic Lift Variation due to Blade Torsional Response (v = 275 km/h)

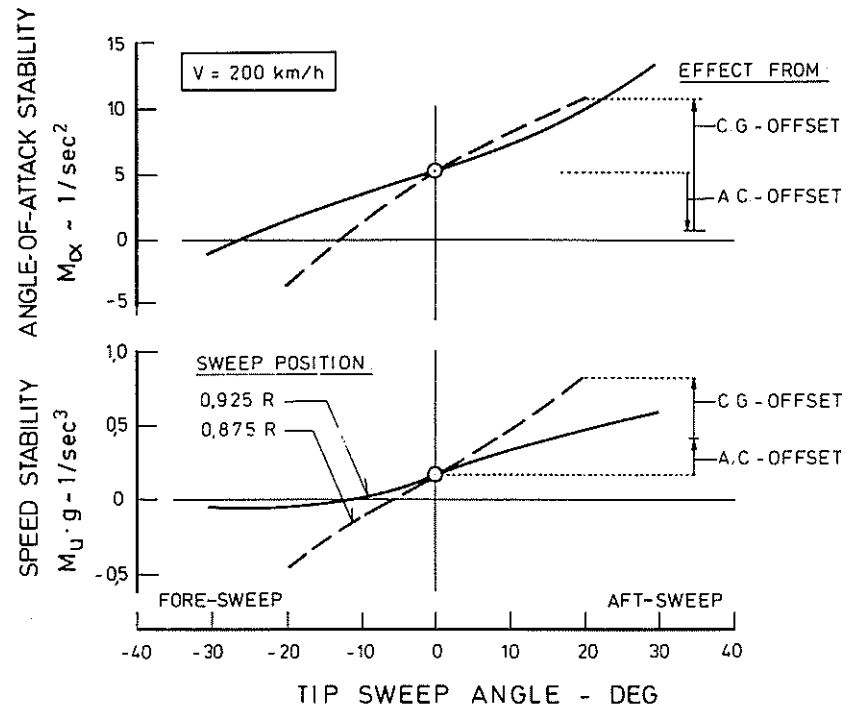

Figure 10 Effect of Tip-Sweep on M_α-, M_u-Derivatives at v = 200 km/h (Constant Tip Chord, Constant Tip Mass, Non-Balanced)

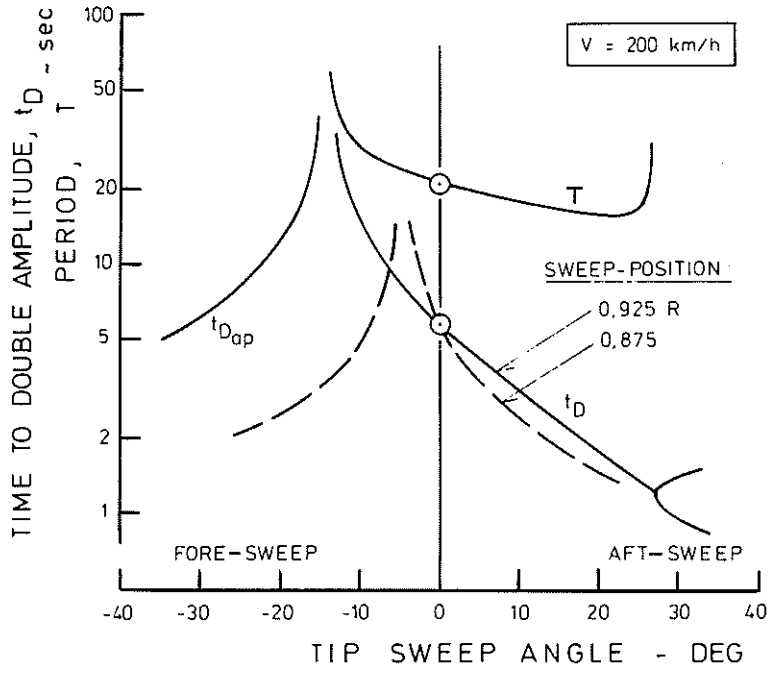

Figure 11 Effect of Tip-Sweep on Dynamic Stability Characteristics at v = 200 km/h (Constant Tip Chord, Constant Tip Mass, Non-Balanced)

NUMBER	VERSION	DESCRIPTIVE PARAMETER
(0)	SB	standard blade
(1)	AGB I	thin-tip (6%)
(2)	AGB III-1	double-swept (30°), thin tip
(3)	AGB III-1	sweep 22°
(4)	AGB III-1	sweep 38°
(5)	AGB III-1	12% airfoil to tip
(6)	AGB III-1	airfoil taper from 0.7 R
(7)	AGB III-1	22,5% c.g. at inboard section
(8)	AGB III-1	21.5% c.g. at inboard section
(9)	AGB III-2	increased tip-weight
(10)	AGB III-2	sweep 22°

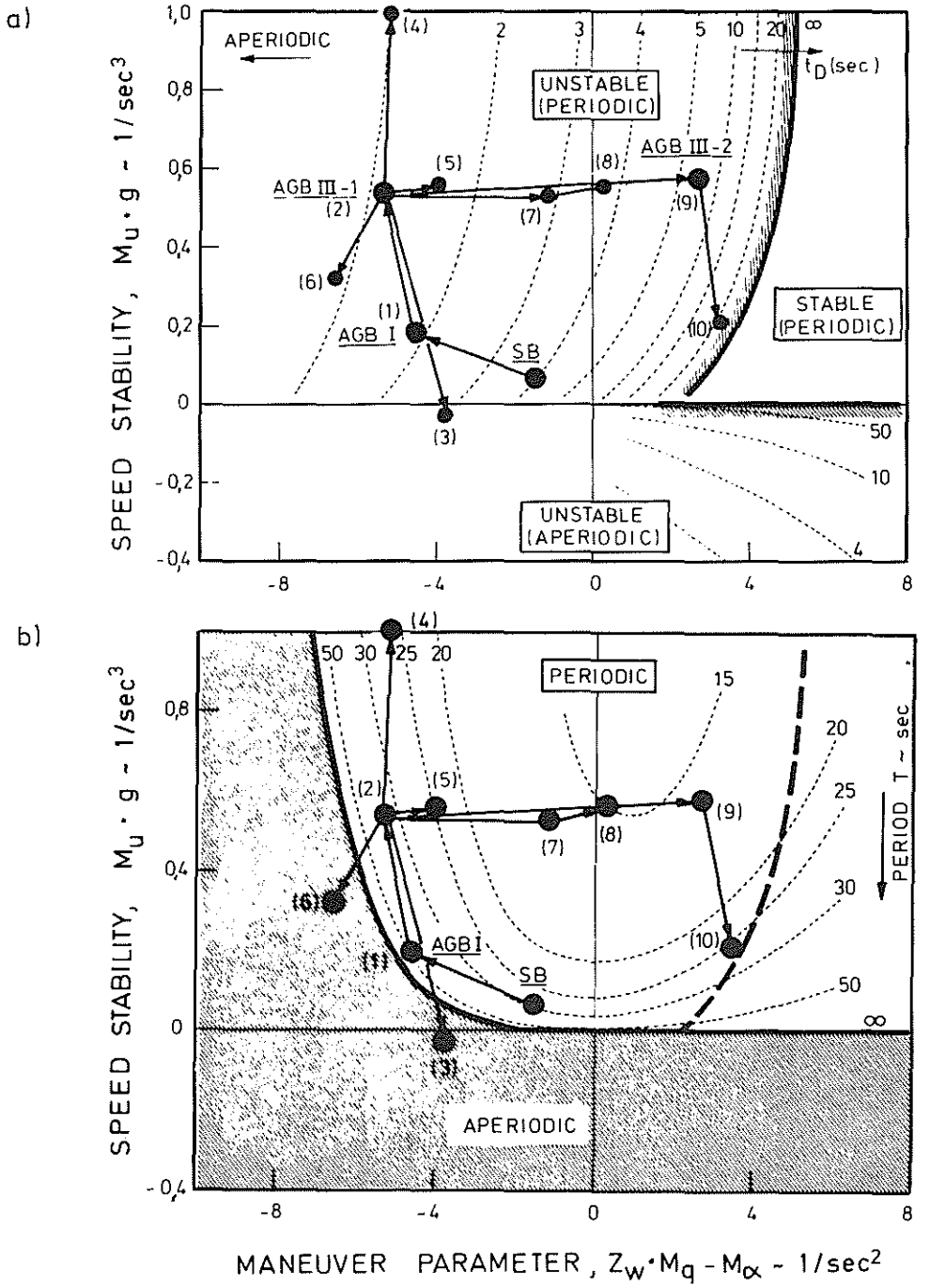

Figure 12 Longitudinal Stability Contributions of Blade Tip Design Parameters (275 km/h)

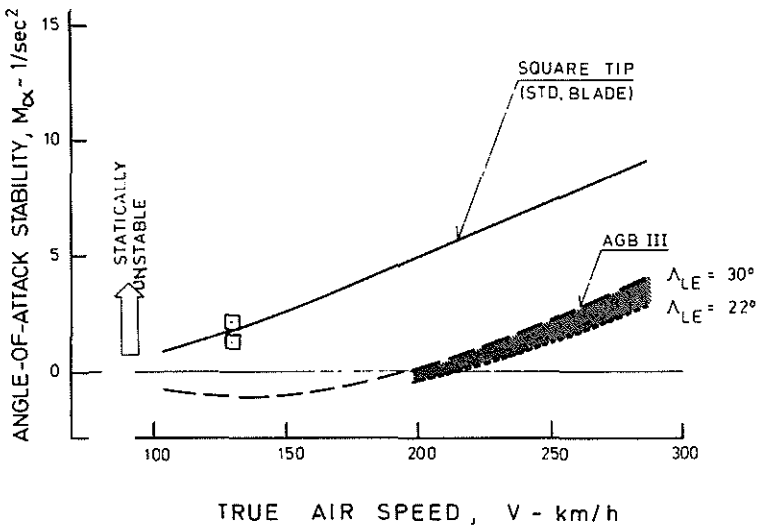

Figure 13 Angle-of-Attack Stability Characteristics versus Speed Range

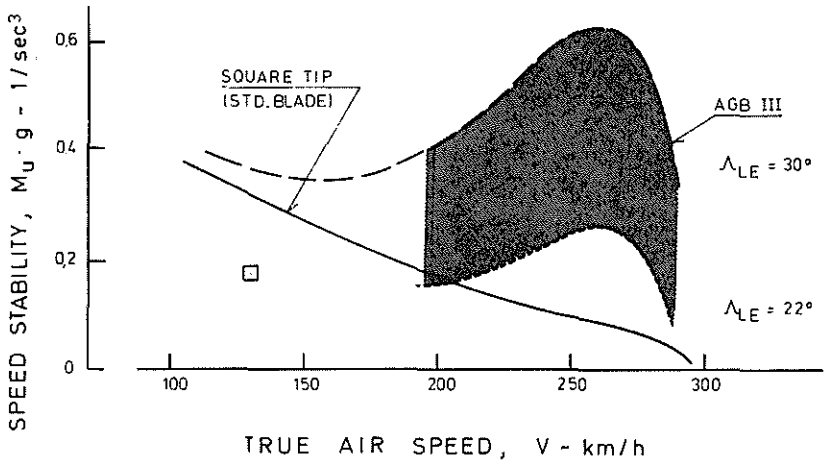

Figure 14 Speed Stability Characteristics versus Speed Range

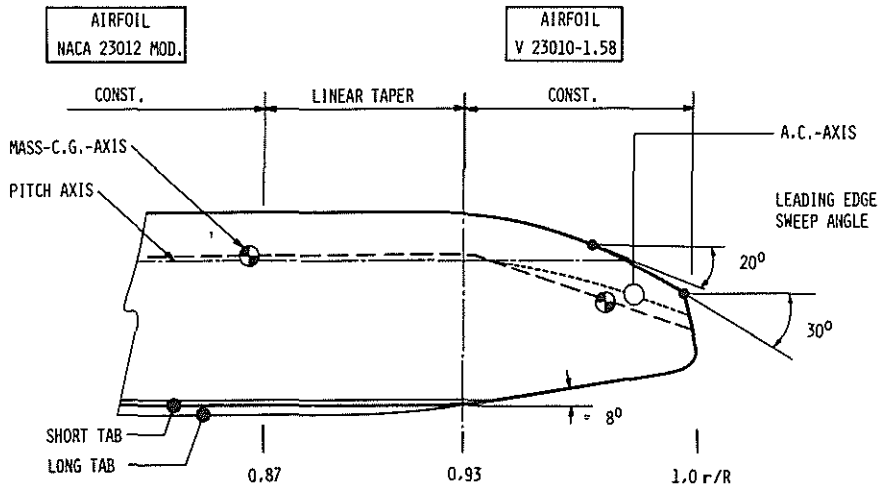

Figure 15 Descriptive Parameters of Advanced Geometry Blade (AGB IV)

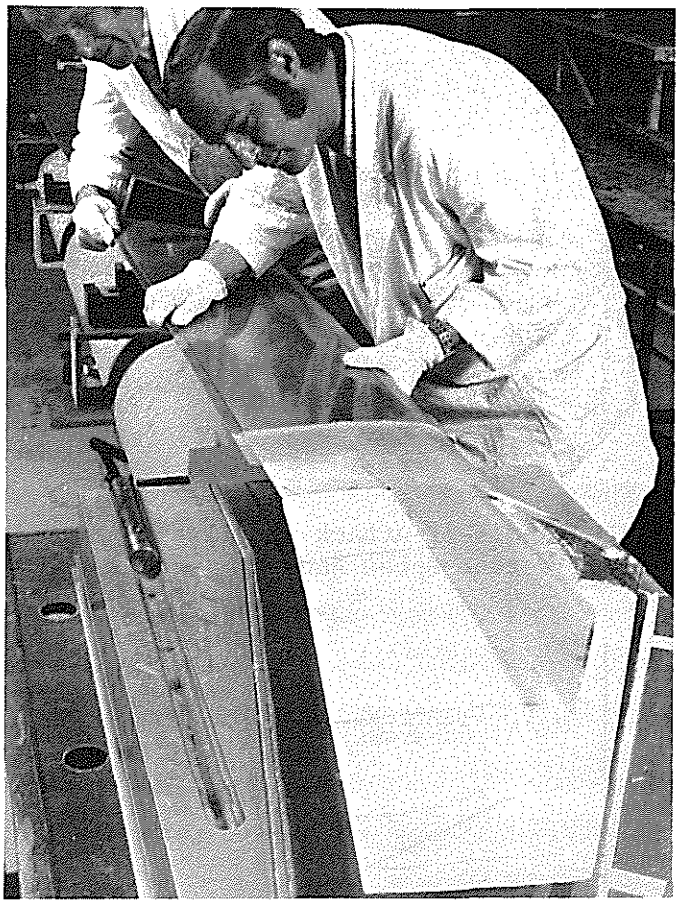

Figure 16 Experimental Manufacturing Process of AGB III Blade Version

			STANDARD BLADE	AGB III	AGB IV
FREQUENCY RATIO	1. FLAP	-	1.117	1.12	1.123
	2. FLAP	-	2.751	2.855	2.758
	3. FLAP	-	4.946	5.31	4.983
FREQUENCY RATIO	1. LAG	-	0.667	0.673	0.688
	2. LAG	-	4.139		4.268
FREQUENCY RATIO	1. TORSION	-	3.7	3.35	3.85
EQUIVALENT HINGE OFFSET (FLAP)			0.14	0.14	0.14
EQUIVALENT HINGE OFFSET (LAG)			0.166	0.168	0.163
BLADE MASS	(a_β)	kg	24.29	24.12	25.10
STATIC MOMENT	(a_β)	mkg	50.80	49.62	50.13
MOMENT OF INERTIA	(a_β)	m^2kg	140.77	134.33	131.79
EQUIVALENT C.G.-POSITION		%c	24.7	≈ 20	24
LOCK-NUMBER		-	3.78	3.96	4.04

Figure 17 Dynamic Characteristics of Different Blade Versions

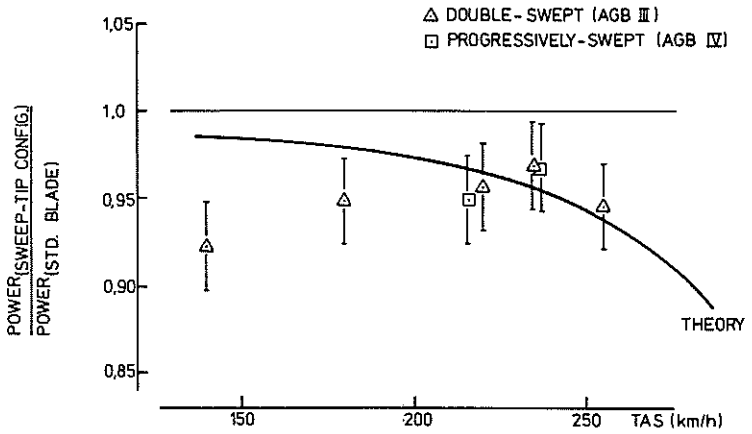

Figure 18 Power Comparison of Different Tip Shapes (GW = 2300 kg, H = 5000 ft)

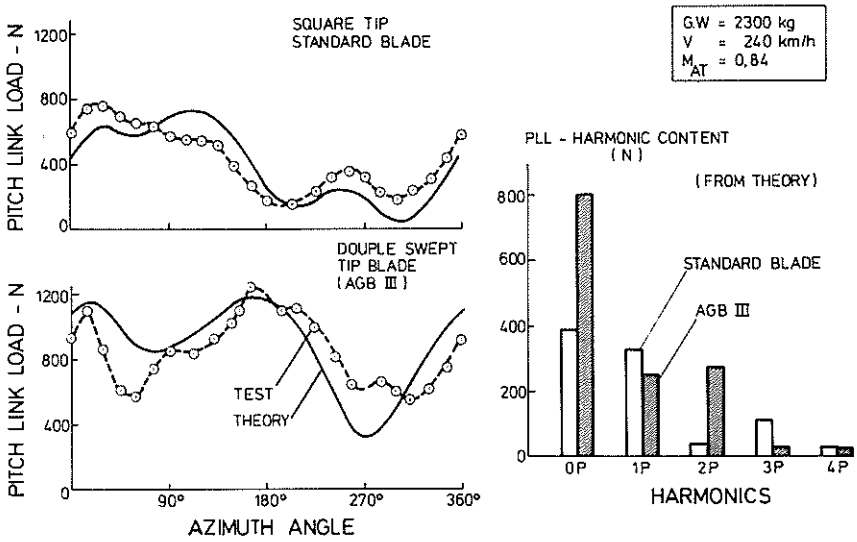

Figure 19 Control Loads Comparison (v = 240 km/h, GW = 2300 kg)

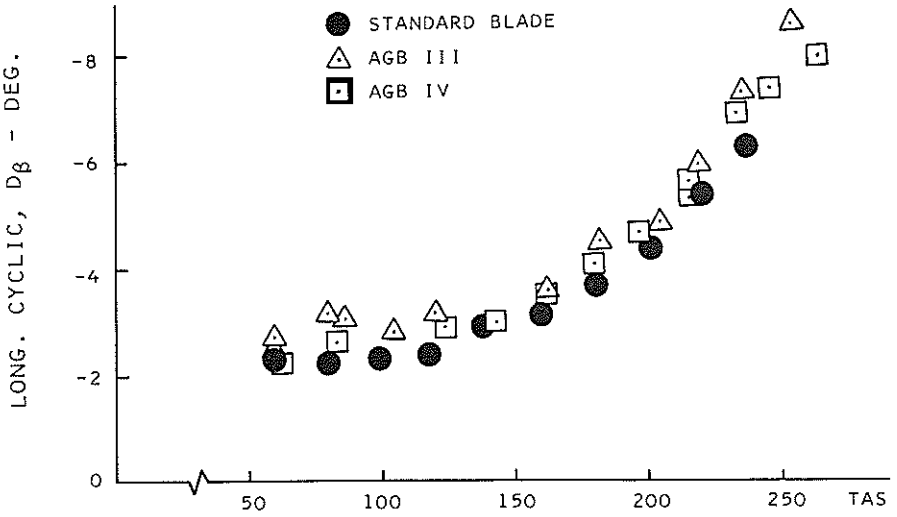

Figure 20 Longitudinal Cyclic Trim for Different Blade Configurations (GW = 2300 kg, X_S = +8 cm)

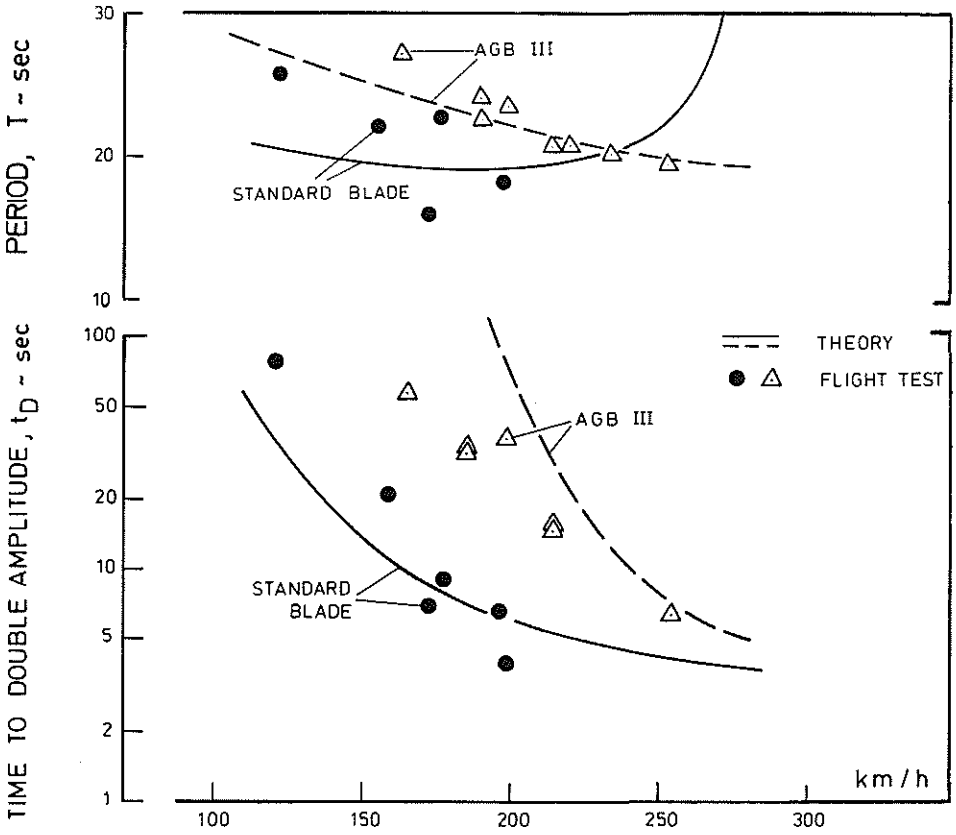

Figure 21 Longitudinal Dynamic Stability (1900 kg, +8 cm, 5000 ft)

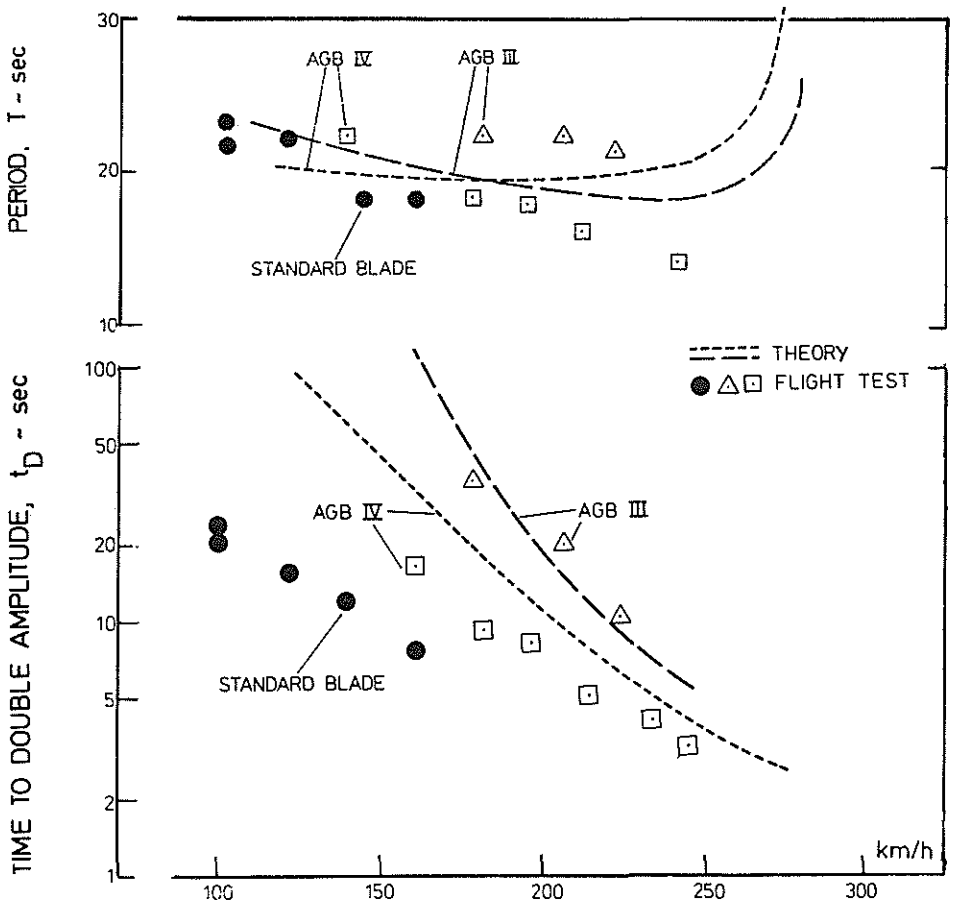

Figure 22 Longitudinal Dynamic Stability (2300 kg, +8 cm, 5000 ft)